

A comprehensive study of parameter determination in a joint MRS and TEM data analysis scheme

Ahmad A. Behroozmand*, Esben Dalgaard, Anders Vest Christiansen and Esben Auken

Department of Geoscience, Aarhus University, Denmark

Received May 2012, revision accepted March 2013

ABSTRACT

We present a comprehensive study of the parameter determination of magnetic resonance sounding (MRS) models in a joint MRS and transient electromagnetic (TEM) data analysis scheme. The parameter determination is assessed by calculating the model parameter uncertainties based on an *a posteriori* model covariance matrix. An entire MRS data set, dependent on pulse moment and time gate values, together with TEM data, is used for all analyses and realistic noise levels are assigned to the data.

Sensitivity analyses are studied for the determination of water content as a key parameter estimated during inversion of MRS data. We show the results for different suites of (three-layer) models, in which we investigate the effect of resistivity, water content, relaxation time, loop side length, number of pulse moments and measurement dead time on the determination of water content in a water-bearing layer. For all suites of models the effect of a top conductive and a top resistive layer are compared. Moreover, we analyse all models for a long (40 ms) and short (10 ms) measurement dead time. The effect of noise level on the parameter determination is also analysed.

We conclude that, in general, the resistivity of the water-bearing layer (layer of interest, LOI) does not affect the determination of water content in the LOI but the resistivity of the top layer increases depth resolution; the water content of the LOI does not influence its determination considerably in cases where the signal has a relatively long relaxation time in the LOI; determination of the water content in the LOI is improved by increasing the relaxation time of the signal in the LOI; short measurement dead time will improve the parameter determination for signals with a relatively short relaxation time; increasing loop side length and the number of pulse moments do not necessarily improve the parameter determination.

INTRODUCTION

Magnetic resonance sounding (MRS), also called surface nuclear magnetic resonance (surface NMR), is an increasingly popular geophysical method for detailed characterization of groundwater resources because of its direct sensitivity to water molecules in the subsurface (e.g., Hertrich 2008). Protons of water molecules are excited at a natural equilibrium state within the Earth's magnetic field. A high-intensity current tuned at the Larmor frequency is passed through a large transmitter loop deployed at the surface. The exciting field tips the magnetization vector away from its equilibrium orientation along the Earth's magnetic field. After switching the current off, the NMR decaying signal (Free Induction Decay, FID) is measured with a wire loop on the surface. MRS data can be inverted with different approaches such as step-wise inversion, which utilizes a fixed MRS kernel consisting in the initial amplitude inversion (Legchenko and Shushakov

1998) or an adaptive MRS kernel during the inversion (Braun and Yaramanci 2008; Braun *et al.* 2009), time-step inversion (Legchenko and Valla 2002; Mohnke and Yaramanci 2005), full-decay (QT) inversion (Müller-Petke and Yaramanci 2010; Behroozmand *et al.* 2012b) and a joint inversion of MRS and TEM/DC data (Behroozmand *et al.* 2012a; Günther and Müller-Petke 2012). As inversion results most often the water content and relaxation time distributions are presented as a function of depth.

Regardless of the inversion method, it is essential to assess the determination of the parameters in the inverted model. In the past there have been a few studies on the resolution of MRS parameters. For instance, Müller-Petke and Yaramanci (2008) studied the resolution of MRS data depending on the loop size, maximum pulse moment and the subsurface resistivity based on singular value decomposition of the MRS forward operator; the trade-off between measurement dead time and relaxation time is described in Dlugosch *et al.* (2011); Legchenko *et al.* (2002) defined the maximum depth of detection as the depth of the top

* ahmad@geo.au.dk

of a 1 m thick infinite horizontal layer of water (100% water content); Günther and Müller-Petke (2012) and Müller-Petke *et al.* (2011) computed parameter uncertainties by variation of individual parameters; Schirov and Rojkowski (2002) and Lehmann-Horn *et al.* (2012) studied the sensitivity of MRS data in the presence of electrical conductivity anomalies; Walsh *et al.* (2011) showed the improved resolution of early-time signals using a shorter measurement dead time.

In this paper, we assess model parameter determination by calculating the parameter uncertainties based on a linearized approximation to an *a posteriori* model covariance matrix. Doing this, we include the full system transfer function, including data noise and system parameters that are crucial in order to obtain reliable uncertainty estimates. The analyses were computed for conductive layered half-spaces. The entire MRS data set (Müller-Petke and Yaramanci 2010; Behroozmand *et al.* 2012b) is used during analyses, rather than initial amplitude data, in order to utilize the full information content of the MRS data. Behroozmand *et al.* (2012a) showed an improvement in MRS parameter determination by joint inversion of MRS and TEM data and discussed the advantage of TEM over DC resistivity (geo-electrics) because of its higher depth penetration. Hence, the analyses in this paper were carried out assuming both MRS and TEM datasets in a full joint implementation.

Since water content is the key MRS parameter to be determined, we focus on the resolution of the water content. Compared to other studies, we carried out sensitivity analyses of many different models of conductive layered half-spaces, varying water contents, resistivities, loop side length, measurement dead time, the number of pulse moments, relaxation time and depth to the water-bearing layer. As to measurement dead time, we analysed for all models those typically obtained from the two commercially available types of MRS equipment (the Numis Poly of IRIS-Instruments and the GMR of Vista Clara Inc.). The rest of the specifications were based on the Numis Poly equipment. Finally, we analysed the effect of noise level on the parameter determination.

METHODOLOGY

In this section we will briefly introduce the implementation of the MRS forward response, noise models and model parameter determination from an *a posteriori* model covariance matrix.

MRS forward modelling

For the forward modelling of MRS data, the entire data set was simulated at different pulse moments (q) and different time gate values (t). A detailed description of the efficient full decay forward modelling of MRS data is presented in Behroozmand *et al.* (2012b). The stretched-exponential (SE) approach (Kenyon *et al.* 1988) approximates the multi-exponential behaviour of the MRS signal and the 1D forward response is given by

$$V(q,t) = \int K(q,z) \cdot W(z) \cdot \exp\left[-\left(\frac{t}{T_2^*(z)}\right)^{C(z)}\right] dz, \quad (1)$$

in which $V(q,t)$ is the entire cube of the measured signal integrated into time windows called 'gate', $K(q,z)$ is the 1D MRS kernel depending on pulse moment and depth, z , and $W(z)$ denotes water content distribution. The SE model is a function of the relaxation time T_2^* and the stretching exponent C at each depth.

Natural noise contribution

In order to give meaning to the sensitivity analysis of MRS data and in order to make the synthetic data comparable with field conditions, we selected all measurement parameters from field data acquired with the NUMIS Poly equipment. The noise contamination is likewise chosen carefully to resemble field conditions:

$$V_{resp} = V + G(0,1) \cdot \left[STD_{uni}^2 + \left(\frac{V_{noise}}{V}\right)^2 \right]^{\frac{1}{2}} \cdot V, \quad (2)$$

where V_{resp} are the perturbed synthetic data; V is the forward response; $G(0,1)$ denotes the Gaussian distribution with a mean value of 0 and a standard deviation of 1; STD_{uni} represents uniform noise added to the data in order to consider non-specified noise contributions like structural noise; V_{noise} is the background noise contribution. For simulation of the MRS synthetic data, the forward response was contaminated by a Gaussian noise distribution with a standard deviation of 64 nV together with a uniform relative

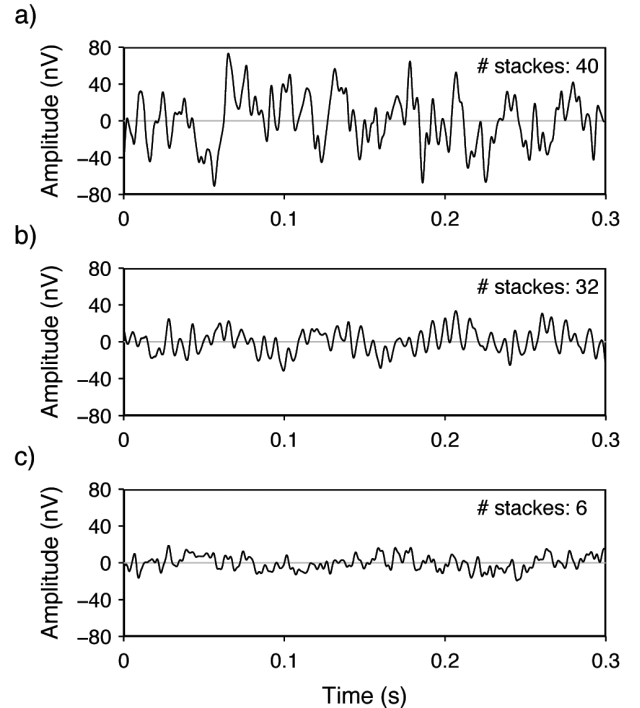


FIGURE 1

Three different noise levels ((a) high noise level, after 40 FIDs stacked together; (b) medium noise level, after 32 FIDs stacked together; (c) low noise level, after 6 FIDs stacked together) detected in the MRS field campaigns in Denmark. The plots show the data errors before gating, which are obtained from imaginary parts of the rotated data.

noise of 3% of the data values, which are assigned to V_{noise} and STD_{uni} in equation (2). The 64 nV noise distribution was applied to the data before gating and the noise on the data was assumed to be uncorrelated. This realistic noise level was assigned to the MRS data to make the analysis results comparable with real field scenarios. In order to illustrate this, Fig. 1 represents three different background noise levels detected in some of our MRS field campaigns in Denmark; a) high noise level, after 40 FIDs stacked together, b) medium noise level, after 32 FIDs stacked together and c) low noise level, after 6 FIDs stacked together. The plots show the data errors before gating that are obtained from the imaginary parts of the rotated data (Müller-Petke *et al.* 2011).

For the TEM data the background noise is given by (Auken *et al.* 2008)

$$V_{noise} = b \cdot \left(\frac{t}{1 \times 10^{-3}} \right)^{-\frac{1}{2}}, \quad (3)$$

in which $b = 3\text{nV}$ is considered as the noise level at 1 ms. In addition, the uniform standard deviation is set to 2% for db/dt responses using a noise calculation similar to equation (2).

Parameter uncertainty estimation

Based on a linear approximation to the *a posteriori* model covariance matrix C_{est} , the estimation of the model parameter uncertainty is given by (Tarantola and Valette 1982; Auken and Christiansen 2004)

$$C_{est} = \left[G^T C_{obs}^{-1} G + C_{prior}^{-1} + R^T C_R^{-1} R \right]^{-1}, \quad (4)$$

where G is the Jacobian matrix of the forward mapping, R is the roughness of the constrained parameters and C_{obs} , C_{prior} and C_R are the covariance matrices of the observed data, the *a priori* information and the roughness constraints. The parameter uncertainty estimates are then obtained by the square root of the diagonal elements of C_{est} . The off-diagonal elements of C_{est} describe the correlation between the model parameters but will not be dealt with in this paper.

For the sensitivity analysis of MRS parameters, few layer 1D models were considered and no *a priori* information was applied to any of the model parameters. Hence, equation (4) becomes:

$$C_{est} = \left[G^T C_{obs}^{-1} G \right]^{-1}. \quad (5)$$

The analyses were carried out on the logarithm of the model parameters, which provides a standard deviation factor STDF, on the parameter m_p , given by

$$STDF(m_i) = \exp\left(\sqrt{C_{est(i,i)}}\right). \quad (6)$$

Therefore, under a lognormal assumption, it is 68% likely that a given model parameter m falls in the interval

$$\frac{m}{STDF_m} < m < m \cdot STDF_m. \quad (7)$$

TABLE 1

Parameter uncertainty intervals and the colours used for analysis.

Degree of parameter determination	STDF Interval	Color
Very well determined	<1.1	
Well determined	1.1-1.2	
Determined	1.2-1.5	
Poorly determined	1.5-2.0	
Very poorly determined	2.0-3.0	
Undetermined	>3.0	

TABLE 2

The basic model used for analyses. Note that for analyses of the model parameters, one of the model parameters varies, as a sweeping parameter, together with depth to the LOI.

Parameter	Layer 1	Layer 2	Layer 3
ρ (Ohm-m)	10 and 100	100	10
W (%)	30	30	30
T_2^* (ms)	20	200	20
C	1	1	1
thk (m)	5-160	10	Inf

This is a good approximation for mildly non-linear problems. We classified the parameter uncertainties in six intervals as stated in Table 1, ranging from $STDF < 1.1$ for very well determined parameters to $STDF > 3.0$ for completely undetermined parameters. Since the calculated uncertainties are based on a linear approximation of the forward mapping, the analysis must be considered qualitatively and not quantitatively, especially for large $STDF$ s.

SYNTHETIC EXAMPLES

For all analyses, a coincident square loop configuration with a side length of 100 m and 1 turn was used for simulating MRS data. The MRS responses (FIDs) consisted of 24 pulse moments distributed between 0.11–13.87 As. A Larmor frequency of 2130 Hz was considered and the Earth's magnetic field was set at an inclination of 70 degrees and a declination of 2 degrees. A 40 ms transmit pulse was used and the FID was calculated in a 500 ms time interval. In order to take the effect of a short measurement dead time in our analyses into account, we considered measurement dead times of both 40 ms (typically used with the Numis Poly/Plus equipment) and 10 ms (relevant to the GMR equipment, Vista Clara Inc.). Relaxation processes during the pulse were not included here.

Based on the assumed noise model, we analysed the uncertainty estimates of the model parameters derived from the model covariance matrix in equation (5).

The basic model consists of three layers; a silty clay top layer underlain by a 10 m aquifer, overlying another silty clay layer at the bottom. Throughout this paper, the second layer is referred to as the layer of interest (LOI).

Table 2 shows the basic model. All layers contain 30% of water while they have relaxation times of 20, 200 and 20 ms, respectively. These relaxation times may correspond to fine, medium to large and fine pore structures (e.g., Schirov *et al.* 1991). A homogeneous layered half-space is assumed so the C value is set to 1 for all layers and is free to change during analyses. We carried out the analyses for both a conductive (10 ohm-m) and a resistive (100 ohm-m) top layer in order to see the effect of conductivity of the top layer.

The parameters of each layer are named as the parameter abbreviation followed by the layer number. For instance, RHO1, W2, T_2^* 3 and THK2 refer to resistivity of the first layer, water content of the second layer, relaxation time of the third layer and thickness of the second layer, respectively.

For simulation of the TEM data, we used the specifications of the WalkTEM instrument, developed at the Department of Geoscience, Aarhus University. It employs a 40 by 40 m square transmitter loop and measures in a dual-moment set-up using a low and a high moment of 1 A and 8 A (magnetic moments of 1600 and 12800 Am²) (Nyboe *et al.* 2010). Current turn-off ramps of 3 microseconds and 5.5 microseconds are assigned to the low- and high-moment current waveforms, respectively. The first data are calculated at a (gate) time of 8.2 microseconds, while the last measurement (gate) time is at 1.4 ms (about 10 gates per decade). The transmitter current waveform is an alternating square wave with 10 ms current on time followed by 10 ms measuring time. A central loop configuration was used for measurements, in which a receiver coil located in the centre of the transmitter loop measures the transient earth response.

The analyses can be done for any 1D model but we will show a few examples giving insight into the resolution capabilities of MRS. We divided the parameters we want to sweep into two groups: the model parameters and the system parameters. We considered the following as the most important model parameters to sweep: resistivity of both the first (RHO1) and second layers (RHO2), water content of both the first (W1) and second layers (W2) and relaxation time of the second layer (T_2^*). We also swept the following system parameters: loop side length (LS), number of pulse moments (# q) and measurement dead time (DT). Moreover, we studied the dependency of the results on different noise levels.

Models 1A and 1B – the effect of resistivity

The first suite of models in our study (model 1A) investigates the effect from varying the resistivity of the LOI (RHO2) on the uncertainty of the water content in the LOI (W2). The model and the analyses are shown in the first column of Fig. 2 (panels a1, b1 and c1). Panel a1 sketches the resistivity model with the fixed parameters shown in black and the sweeping parameters in red. The depth to the LOI sweeps from 5–160 m in 14 steps while RHO2 sweeps between 1–1000 ohm-m in 7 steps. The same sweeping values of depth to the LOI are used for all mod-

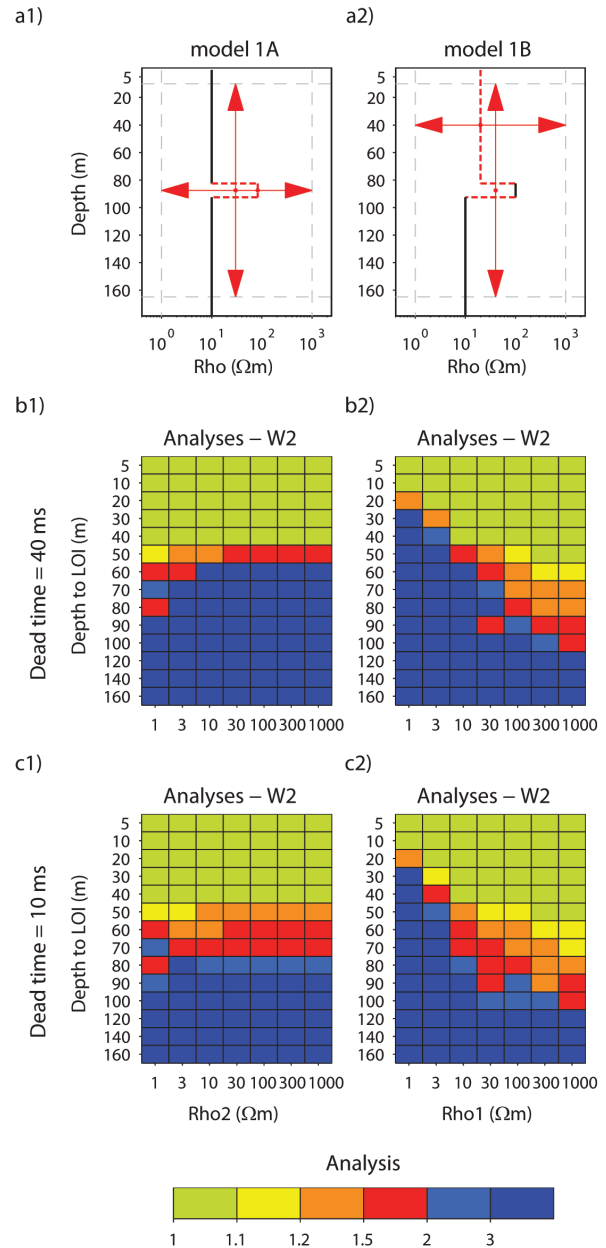


FIGURE 2 Sensitivity analyses for models 1A (the effect of RHO2) and 1B (the effect of RHO1). Panels a1 and a2 sketch the resistivity models. Dashed red lines show the sweeping parameters, while fixed parameters are shown with solid black lines. Red arrows show the sweeping intervals. The rest of the parameters are as stated in Table 2. The results present resolution of the parameter W2 in colours; see the legend and Table 1. The panels in rows 2 and 3 show analyses of the same models for different measurement dead times of 40 ms and 10 ms, respectively. For site specifications see the text.

els. The total number of analysed models in Fig. 2 thus consists of $14 \times 7 = 98$ models. The remaining model parameters are as given in Table 2.

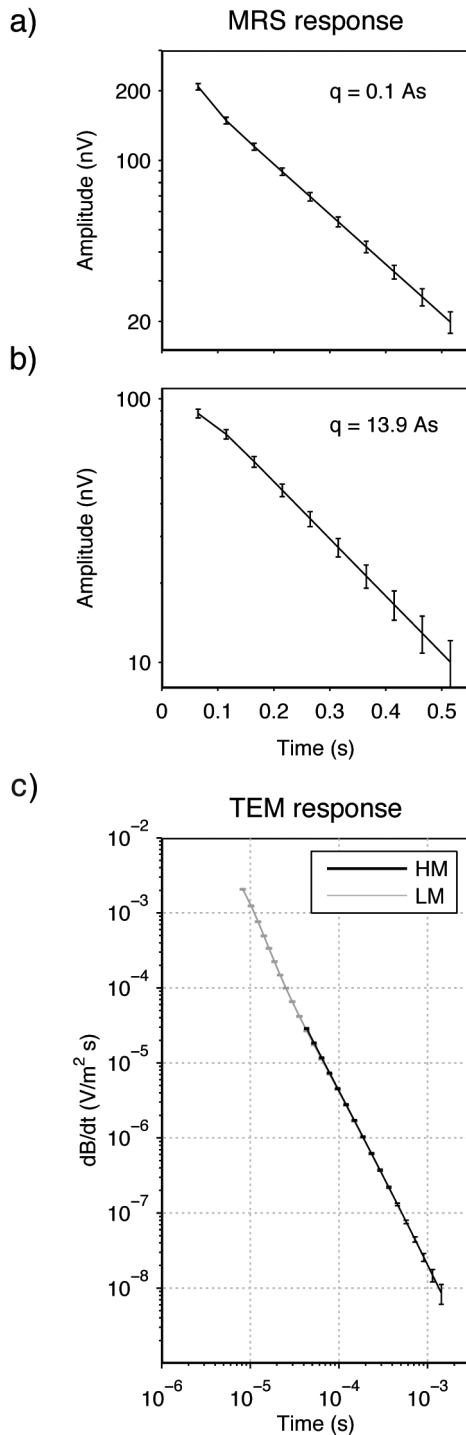


FIGURE 3
 An example of MRS and TEM responses used in sensitivity analyses, together with their standard deviation. The responses are simulated for the model containing $\text{RHO}2 = 100 \text{ ohm-m}$ and depth to the LOI of 5 m in Fig. 2, panel b1 (depicted in column 5 and row 1). (a,b) The MRS forward responses for $q = 0.1 \text{ As}$ and $q = 13.9 \text{ As}$. c) The TEM forward response in dB/dt for the low-moment (grey) and high-moment data (black).

The results are shown as colour boxes, changing from green (very well determined parameter, $\text{STDF} < 1.1$) to dark blue (completely undetermined parameter, $\text{STDF} > 3.0$). In the b panels (b1 and b2) the dead time is 40 ms while for the c panels (c1 and c2) it is only 10 ms. If we use the terms given in Table 1, all parameters' uncertainties shown in warm colours are resolved to a given degree, while uncertainties shown in cold colours are unresolved. In panel b1, the analyses show that the resistivity of the water-bearing layer (LOI) has a negligible effect on the resolution of W2. A slight improvement is observed for $\text{RHO}2$ s of 1 and 3 ohm-m in deep parts, which is due to a better TEM resolution of these very conductive layers. Larger resistivity values have no influence on the determination of W2. The latter was also concluded by Braun and Yaramanci (2008). W2 is very well determined (green colour) down to 40 m for all models, well to poorly determined at a depth of 50 m and almost undetermined afterwards. Panel c1, with a dead time of only 10 ms, generally matches the results in panel b1, except that the lower boundary of the resolved structure moves deeper to depths of 70 m.

Considering the site specifications, i.e., loop size etc., a relatively shallow part of the structure (down to 40 m) is very well determined (green colour) in panels b1 and c1, which is due to the high conductivity of the top layer ($\text{RHO}1 = 10 \text{ ohm-m}$).

In order to investigate the effect of the resistivity of the top layer, panels b2 and c2 in Fig. 2 have $\text{RHO}1$ as the sweeping parameter. Panel a2 shows the resistivity model. The resistivity $\text{RHO}1$ varies between 1–1000 ohm-m and $\text{RHO}2$ is set to 100 ohm-m. Increasing the resistivity of the top layer increases the resolution at depth as expected, forming a sloped feature for the resolved parameters as shown in panel b2. The lower boundary of the resolved structure varies from 20 m for $\text{RHO}1$ of 1 ohm-m down to 100 m for $\text{RHO}1$ of 1000 ohm-m. Panel c2 shows about the same as panel b2 indicating that the dead time in this case has little influence on the model parameter determination.

It is noteworthy that analyses of both models 1A and 1B represent identical structures of very well determined parameters (green colour) in rows b) and c) (comparing panels b1 and c1 and panels b2 and c2). In other words, for these two suites of models, the measurement dead times of 10 ms and 40 ms lead to the same analysis of very well determined parameters. This is explained by the high-relaxation time in the LOI (200 ms), meaning that the FID is long enough to be characterized properly anyway. We will show this effect later in models 3A and 3B.

For completeness we show an example of the MRS and TEM data together with their standard deviation in Fig. 3. The responses assume $\text{RHO}2 = 100 \text{ ohm-m}$ and a depth to the LOI of 5 m (the model in column 5 and row 1 in panel b1). Panels a and b show the MRS response on a logarithmic scale for small (0.1 As) and large (13.9 As) pulse moments and the corresponding noise on the data. The TEM response is shown in panel c. The low-moment (LM) data are shown in grey, while black represents the high-moment (HM) data.

Models 2A and 2B – the effect of water content

Model 2A studies the effect of water content (in the LOI, W2) on its resolution. The water content model is sketched in Fig. 4, panel a1. The water content of the first and third layers was set to 30% and W2 varied between 5–45% (9 values, equally spaced). Therefore, each panel of the analyses contains $14 \times 9 = 126$ analysed models. Resistivity values of 10, 100 and 10 ohm-m were assigned to the layers and the rest of the parameter values were as stated in Table 2. As a main result of these model analyses, the water content of the LOI does not considerably influence how well it is determined. Again this is mainly due to the high relaxation time in the LOI (200 ms) and the low-relaxation times (20 ms) in the other layers. The results are shown in panel b1. The estimated W2 is well determined down to 40 m (due to the top conductive layer), poorly determined at a depth of 50 m and undetermined afterwards.

As panel c1 shows, a decreasing measurement dead time provides more information in the depth interval from 50–80 m. However, similar to panel b1, the effect of W2 on its resolution is negligible for well determined parts of the structure.

Column 2 of Fig. 4 deals with model 2B for which the water content of the top layer varies as the sweeping parameter, as sketched in panel a2. The same values, as in model 2A, between 5–45% were considered for W1 and W2 was set to 30%. The rest of the parameters were set to their values as in model 2A. Variation of W1 has no influence on the determination of parameter W2, as shown in panel b2. This is due to a short relaxation time (20 ms) of the top layer, i.e., for the considered range of W1 the contribution of the top layer to the FIDs vanishes before the measurement starts. For a measurement dead time of 10 ms (panel c2), the same analysis structure is observed and more depth information is provided.

Similar to models 1A and 1B, the depth resolution of the well determined part of the structure is not improved by decreasing the measurement dead time because of a relatively high-relaxation time of the LOI.

Models 3A and 3B – the effect of relaxation time

The last suite of analysed models with sweeping model parameters considers the effect of the relaxation time of the LOI (T_2^{*2}) on the resolution of W2. Panel a1 in Fig. 5 shows the resistivity models. The layers have resistivity values of 10, 100 and 10 ohm-m, respectively. All layers contain a water content of 30% and the rest of the parameters follow the values in Table 2. The sweeping parameters are depth to the LOI and the relaxation time of the LOI that varies between 20–300 ms (9 values), i.e., form different contexts from a very fine pore structure (silty clay) to a large pore structure (coarse sand and gravel) (Schirov *et al.* 1991). Hence, $14 \times 9 = 126$ models were analysed in each panel. In panel b1, i.e., considering a measurement dead time of 40 ms, the very well determined structure (green colour) starts from a T_2^{*2} value of 75 ms. Nothing is resolved for a relaxation time of 20 ms even at shallow depths. As expected, increasing the

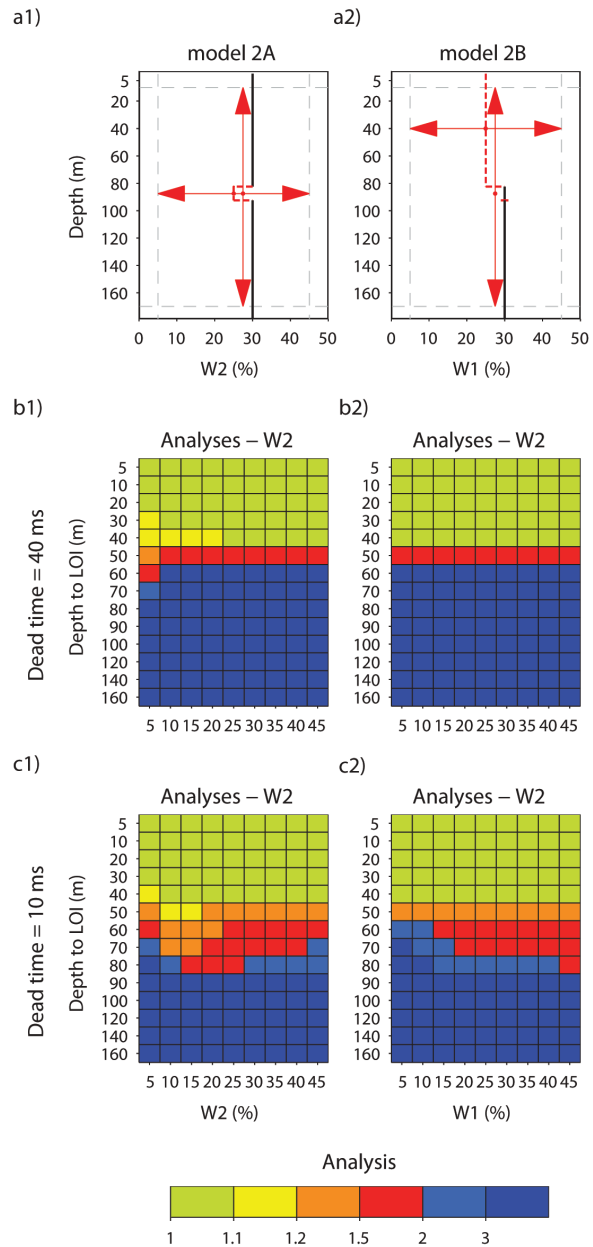


FIGURE 4 Sensitivity analyses for models 2A (the effect of W2) and 2B (the effect of W1). Panels a1 and a2 sketch the water content models. Dashed red lines show the sweeping parameters, while fixed parameters are shown with solid black lines. Red arrows show the sweeping intervals. The rest of the parameters are as stated in Table 2. The results present resolution of the parameter W2 in colours; see the legend and Table 1. The panels in rows 2 and 3 show analyses of the same models for different measurement dead times of 40 ms and 10 ms, respectively. For site specifications see the text.

relaxation time at the LOI will improve the determination of W2 both at shallow intervals and at larger depths. Both relaxation times of 200 and 300 ms (two last columns) represent identical parameter determination. The same feature of improvement in

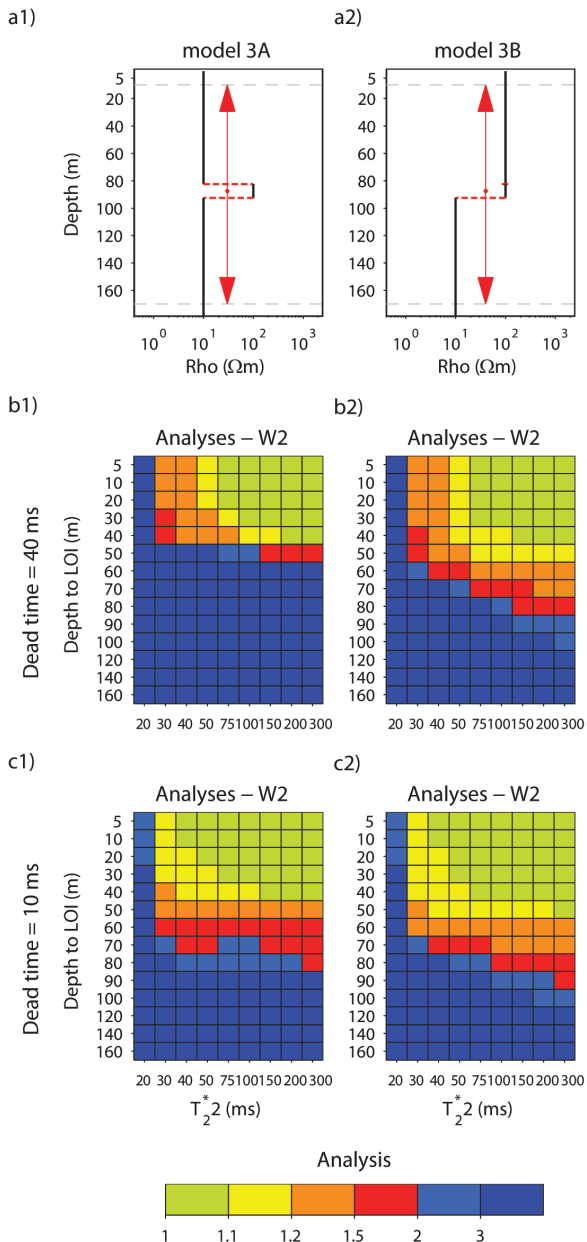


FIGURE 5

Sensitivity analyses for models 3A and 3B, both showing the effect of T_2^* . The models differ in resistivity of the top layer. Panels a1 and a2 sketch the resistivity models. Dashed red lines show the sweeping parameters, while fixed parameters are shown with solid black lines. Red arrows show the sweeping intervals. The rest of the parameters are as stated in Table 2. The results present resolution of the parameter W2 in colours; see the legend and Table 1. The panels in rows 2 and 3 show analyses of the same models for different measurement dead times of 40 ms and 10 ms, respectively. For site specifications see the text.

W2 determination is seen in panel c1 in which the measurement dead time is set to 10 ms. Compared to panel b1, the parameter determination is improved considerably for short relaxation

times, which is due to the shorter measurement dead time. Moreover, improved depth information is obtained when decreasing the dead time and the lower boundary of the resolved structure moves down from 50 m to 80 m.

Column 2 in Fig. 5 shows model 3B together with the analyses. The model differs from model 3A in terms of resistivity of the top layer, which is increased to 100 ohm-m. Compared to panel b1, depth resolution is significantly improved in panel b2 because of the high resistivity of the top layer. This effect is more pronounced for long T_2^* values. Similar to the results in panel c1, a shorter measurement dead time improves the results, particularly for short T_2^* values (panel c2). Improvement with depth of the resolved structure is less pronounced here compared to model 3A where the top layer is conductive.

In summary, the short measurement dead time highly improves parameter determinations especially for signals with a short relaxation time. Improvement in parameter determination at larger depths is largest when a top resistive layer exists.

The next three synthetic models present the effect of system parameters on the determination of W2.

Models 4A and 4B –the effect of loop side length

In this part, we study the effect of the parameter loop side length on the determination of parameter W2. These analyses were carried out to investigate how the resolution and depth information are improved by enlarging the loop. The results are shown in Fig. 6. The resistivity models (panels a1 and a2) are the same as in Fig. 5, i.e., resistivity values of 10, 100 and 10 ohm-m from top to bottom and other parameters are as stated in Table 2. Loop side length values of 25, 50, 75, 100 and 150 m were considered for the analyses, which form $14 \times 5 = 70$ analysed models in each panel. For a measurement dead time of 40 ms, increasing the loop side length does not necessarily improve the determination of W2 as shown in Fig. 6, panel b1. This matter is also highlighted in Müller-Petke and Yaramanci (2008). Depth information is improved by increasing the loop side length up to 75 m, while no considerable improvement is achieved by further increasing the loop side length from 75 m to 150 m. The same behaviour is observed when decreasing the dead time to 10 ms (panel c1), except that, most importantly, depth resolution is improved and the lower boundary of the resolved structure moves down to 80 m. Note that the estimation of the very well determined structure (green part) does not depend on the measurement dead time. Similar to panel b1, the parameter W2 is almost equally determined for loop side lengths of 75, 100 and 150 m. This is an interesting result that helps to save time and effort in the field and makes MRS sounding possible in a more confined space without loss of information.

For the case of the top resistive layer (model 4B, column 2), depth information is generally improved by increasing the loop side length, for both long (40 ms, panel b2) and short (10 ms, panel c2) dead times. In addition, a slight improvement of infor-

mation on depth is achieved when employing the shorter dead time but very well resolved parameters (green colour) are determined as well as in panel b2.

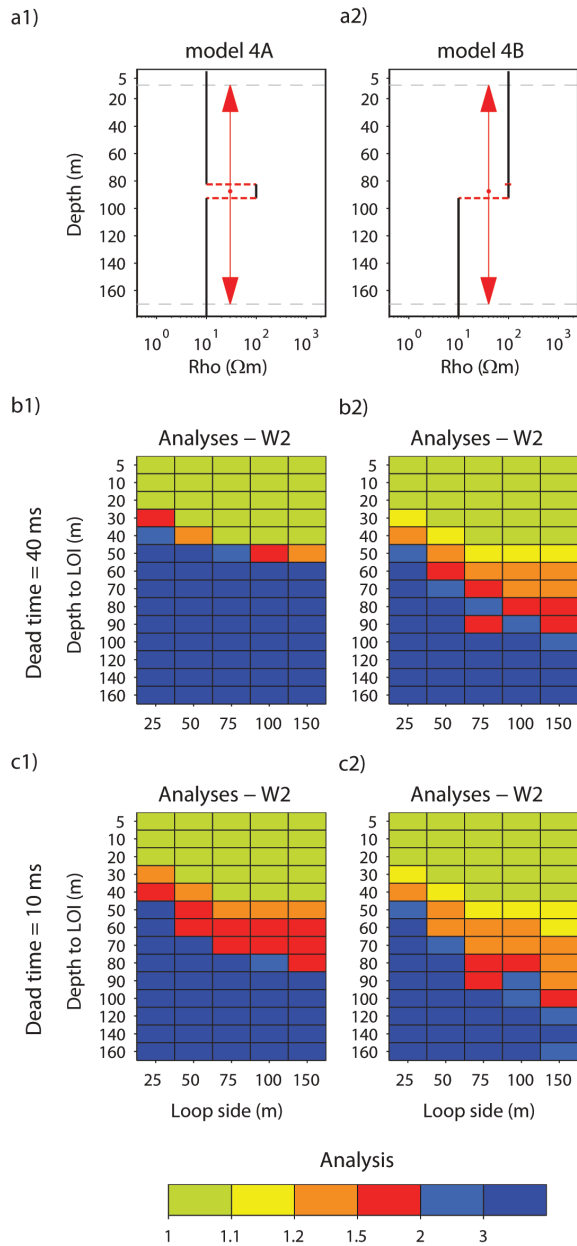


FIGURE 6 Sensitivity analyses for models 4A and 4B. Both show the effect of loop side length. The models differ in resistivity of the top layer, as sketched in panels a1 and a2. Dashed red lines show the sweeping parameters, while fixed parameters are shown with solid black lines. Red arrows show the sweeping intervals. The rest of the parameters are as stated in Table 2. The results present resolution of the parameter W2 in colours; see the legend and Table 1. The panels in rows 2 and 3 show analyses of the same models for different measurement dead times of 40 ms and 10 ms, respectively. For site specifications see the text.

It should be mentioned that the noise levels were scaled with the loop size. Furthermore, it is noteworthy that these results are obtained by considering the same q_{max} for all loop sizes, which does not exactly occur in a real case. It means that the instrument limitation in sending an identical maximum current for different loop sizes was not taken into account.

Models 5A and 5B – the effect of measurement dead time

In this part, we sweep the measurement dead time together with the depth to the LOI. Five values of 5, 10, 20, 30 and 40 ms were assigned to the measurement dead times, forming $14 \times 5 = 70$ analysed models in each panel, as shown in Fig. 7. Similar resistivity models as in Fig. 5 are used and the rest of the parameters follow the values in Table 2. In the case of a top conductive layer (panel b1), depth resolution is generally weakened by increasing the dead

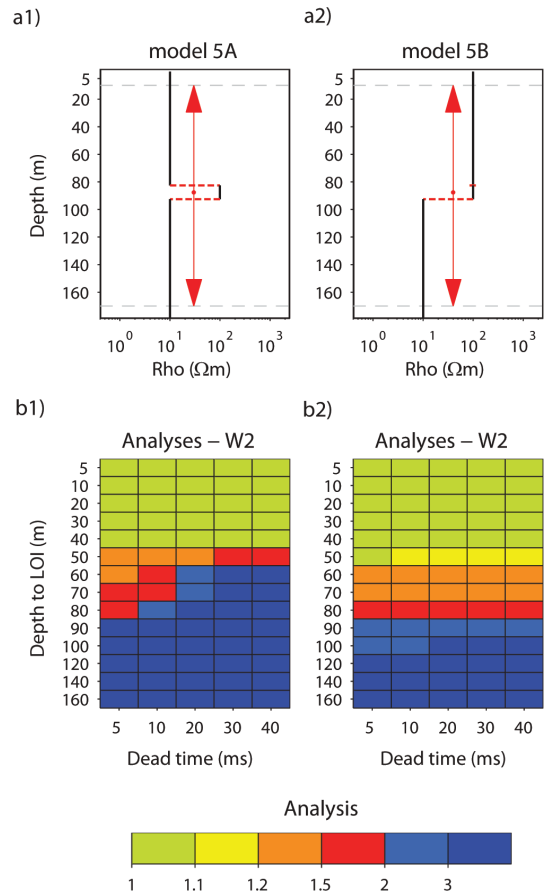


FIGURE 7 Sensitivity analyses for models 5A and 5B. Both show the effect of measurement dead time. The models differ in resistivity of the top layer. Panels a1 and a2 sketch the resistivity models. Dashed red lines show the sweeping parameters, while fixed parameters are shown with solid black lines. Red arrows show the sweeping intervals. The rest of the parameters are as stated in Table 2. The results present resolution of the parameter W2 in colours; see the legend and Table 1. For site specifications see the text.

time value up to 30 ms and the same resolutions are achieved for dead time values of 30 and 40 ms. It should be noted that for model 5A, the very well determined part of the structure (green colour) does not vary for the given dead time values. This is due to the fact that a long relaxation time of 200 ms in the LOI allows characterizing the FIDs even if long dead time values are applied.

For the case of a top resistive layer (panel a2), no significant improvement is observed (panel b2) but the depth resolution is increased as expected. Through the structure, closely identical estimates of W2 are achieved for all dead time values.

The results of this analysis underline the importance of the measurement dead time for the resolution of a given model.

Models 6A and 6B – the effect of the number of pulse moments

This suite of synthetic models deals with the effect of the number of pulse moments q , which is the product of current amplitude and pulse duration. Müller-Petke and Yaramanci (2008) studied the effect of q_{max} itself. The number of pulse moments is one of the key parameters determining the total time it takes to perform a full sounding. During a measurement, a series of increasing pulse moments provide depth information. In addition, pulse moments need to be sampled densely enough in order to provide sufficient resolution of the subsurface when calculating the MRS kernel. The aim of studying models 6A and 6B is to find the sufficient number of pulse moments required for the best model parameter determination of a given model. In other words, to investigate how increasing the number of pulse moments increases the determination of model parameters (here W2). The same resistivity models as in Fig. 5 are considered as shown in Fig. 8 (panels a1 and a2) and the rest of the parameters are as stated in Table 2. Seven values of 2, 4, 8, 12, 16, 20 and 24 are considered as the number of pulse moments # q , which are spaced between pulse moment values of 0.11 and 13.87 As. Therefore, $14 \times 7 = 98$ analysed models are investigated in each panel. Panel b1 shows that the determination of W2 is improved by increasing # q up to 16. After this, almost no increase in the resolution is achieved by increasing # q . Decreasing dead time (panel c1) will increase depth information as seen for other models and, like in panel b1, closely identical determination of W2 is obtained for # q of 16, 20 and 24.

In the case of a top resistive layer (model 6B, column 2), the analyses result in the same conclusion as for model 6A, meaning that 16 pulse moments are sufficient for determination of W2 in the given models. Taking advantage of this knowledge, the time saved is 33% on this model, compared to using 24 pulse moments. Note that the sufficient number of pulse moments might change for different models but increasing the number of pulse moments does not necessarily increase the parameter determination. This matter is also highlighted in Legchenko and Shushakov (1998).

The effect of noise level

This last suite of synthetic models investigates the influence of noise level on the parameter determination. We repeated the

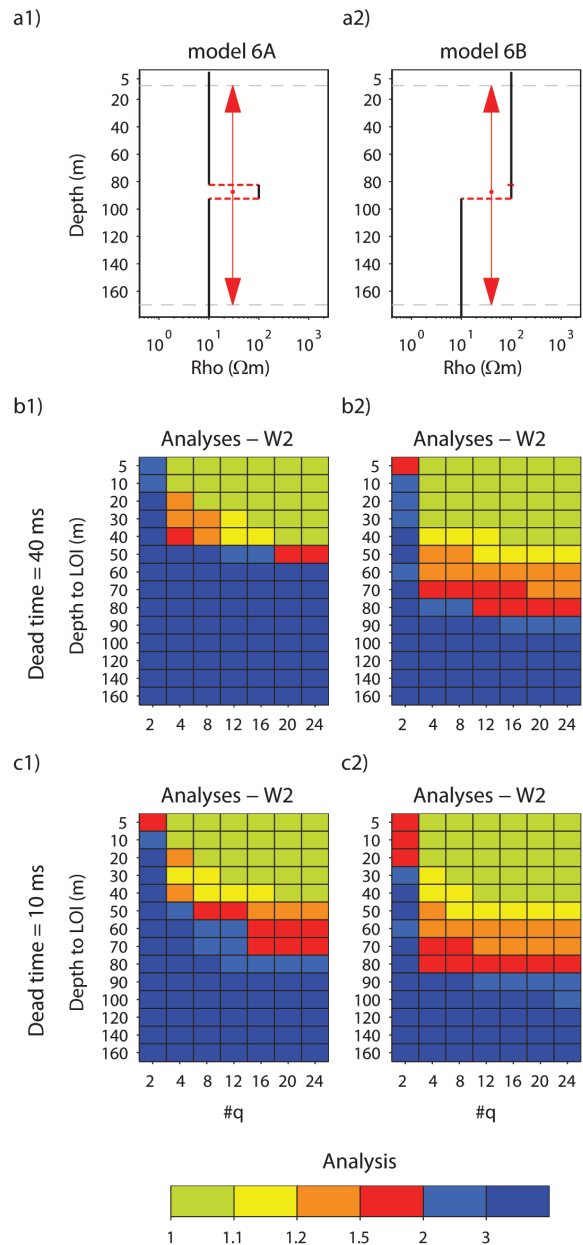


FIGURE 8

Sensitivity analyses for models 6A and 6B. Both show the effect of the number of pulse moments # q . The models differ in resistivity of the top layer, as sketched in panels a1 and a2. Dashed red lines show the sweeping parameters, while fixed parameters are shown with solid black lines. Red arrows show the sweeping intervals. The rest of the parameters are as stated in Table 2. The results present resolution of the parameter W2 in colours; see the legend and Table 1. The panels in rows 2 and 3 show analyses of the same models for different measurement dead times of 40 ms and 10 ms, respectively. For site specifications see the text.

analyses of model 3B (panel b2 in Fig. 5) considering different background noise levels of 16, 64 and 256 nV in equation (2). The results are shown in Fig. 9. The same resistivity and MRS

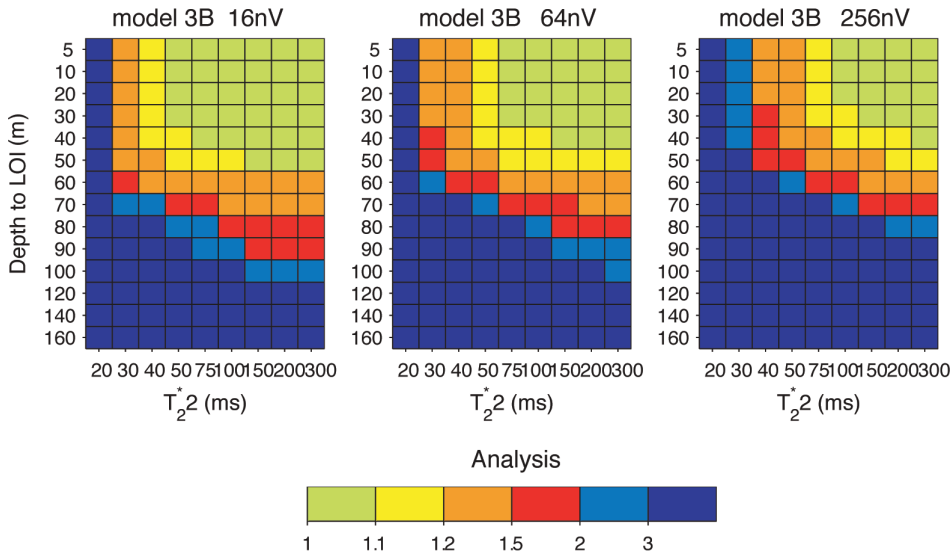


FIGURE 9 Influence of noise level on the parameter determination. The analyses were repeated for model 3B (panel b2 in Fig. 5) considering different background noise levels of 16 (left), 64 (middle, the same as panel b2 in Fig. 5) and 256 nV (right) in equation (2). The rest of the parameters are as stated in Fig. 5 column 2. The results present resolution of the parameter W2 in colours; see the legend and Table 1. For site specifications see the text.

parameters as in Fig. 5 column 2 are used for analyses. As clearly seen, increasing the noise level weakens the parameter determination over the x-axis (T_2^*) and in depth.

CONCLUSION

We studied the parameter determination of MRS models in a joint application of MRS and TEM data. The analyses are presented for many different models in which the effects of the model and the system parameters on the determination of water content are investigated. These parameters consist in resistivity, water content, relaxation time, loop side length, number of pulse moments and measurement dead time. The results are compared for cases of both a conductive and a resistive top layer and for two measurement dead times of 40 ms and 10 ms, which are typically obtained with the two kinds of commercially available MRS equipment. Moreover, we showed the effect of noise level on the parameter determination.

As the main results of the investigated models, the resistivity of the water-bearing layer (LOI) has a negligible effect on the resolution of W2, whereas increasing resistivity of the top layer increases the resolution at depth as expected (Fig. 2). The water content of the LOI does not influence its determination considerably and variation of W1 has no influence on the determination of W2 (Fig. 4). Increasing T_2^* will improve the determination of W2 both at shallow intervals and at larger depths and depth resolution is significantly improved when a top resistive layer exists (Figs 5b1 and 5b2). Moreover, the parameter determination is considerably improved for short relaxation times (Figs 5c1 and 5c2). This highlights the effect of a short measurement dead time for signals with a short relaxation time. Increasing the loop side length does not necessarily improve the determination of W2 (Figs 6b1 and 6c1). The same result is concluded in the case of a resistive top layer (model 4B), except that the depth information is improved (Figs 6b2 and

6c2). A short measurement dead time will improve the parameter determination if the signal has a relatively short relaxation time in the LOI (Figs 5 and 7). Increasing the number of pulse moments does not necessarily improve the parameter determination (Fig. 8).

For given geological information of the measurement site, a pre-survey analysis will help to optimize the measurement time and the resolution of model parameters.

ACKNOWLEDGEMENTS

This work was carried out as part of the Danish Council of Strategic Research Project titled ‘HyGEM – Integrating geophysics, geology, and hydrology for improved groundwater and environmental management’, the RiskPoint project (Assessing the Risks Posed by Point Source Contamination to Groundwater and Surface Water Resources, grant number 09-063216) and NICA (Nitrate Reduction in Geologically Heterogeneous Catchments), the two latter projects supported by the Danish Agency for Science Technology and Innovation. We would also like to thank Nikolaj Foged and Gianluca Fiandaca, Aarhus University, for many useful discussions during the work with the analyses. We would like to thank two anonymous reviewers whose fruitful comments helped improve the clarity of this paper.

REFERENCES

Auken E. and Christiansen A.V. 2004. Layered and laterally constrained 2D inversion of resistivity data. *Geophysics* **69**, 752–761.
 Auken E., Christiansen A.V., Jacobsen L. and Sørensen K.I. 2008. A resolution study of buried valleys using laterally constrained inversion of TEM data. *Journal of Applied Geophysics* **65**, 10–20.
 Behroozmand A.A., Auken E., Fiandaca G. and Christiansen A.V. 2012a. Improvement in MRS parameter estimation by joint and laterally constrained inversion of MRS and TEM data. *Geophysics* **74**, WB191–WB200.

- Behroozmand A.A., Auken E., Fiandaca G., Christiansen A.V. and Christensen N.B. 2012b. Efficient full decay inversion of MRS data with a stretched-exponential approximation of the T2* distribution. *Geophysical Journal International* **190**, 900–912.
- Braun M., Kamm J. and Yaramanci U. 2009. Simultaneous inversion of magnetic resonance sounding in terms of water content, resistivity and decay times. *Near Surface Geophysics* **7**, 589–598.
- Braun M. and Yaramanci U. 2008. Inversion of resistivity in Magnetic Resonance Sounding. *Journal of Applied Geophysics* **66**, 151–164.
- Dlugosch R., Mueller-Petke M., Günther T., Costabel S. and Yaramanci U. 2011. Assessment of the potential of a new generation of surface nuclear magnetic resonance instruments. *Near Surface Geophysics* **9**, 89–102.
- Günther T. and Müller-Petke M. 2012. Hydraulic properties at the North Sea island Borkum derived from joint inversion of magnetic resonance and electrical resistivity sounding. *Hydrology and Earth System Sciences Discussions* **9**, 2797–2829.
- Hertrich M. 2008. Imaging of groundwater with nuclear magnetic resonance. *Progress in Nuclear Magnetic Resonance Spectroscopy* **53**, 227–248.
- Kenyon W.E., Day P.I., Straley C. and Willemsen J.F. 1988. Three-part study of NMR longitudinal relaxation properties of water-saturated sandstones. *SPE Formation Evaluation* **3**, 622–636.
- Legchenko A., Baltassat J.M., Beauce A. and Bernard J. 2002. Nuclear magnetic resonance as a geophysical tool for hydrogeologists. *Journal of Applied Geophysics* **50**, 21–46.
- Legchenko A.V. and Shushakov O.A. 1998. Inversion of surface NMR data. *Geophysics* **63**, 75–84.
- Legchenko A. and Valla P. 2002. A review of the basic principles for proton magnetic resonance sounding measurements. *Journal of Applied Geophysics* **50**, 3–19.
- Lehmann-Horn J.A., Hertrich M., Greenhalgh S.A. and Green A. G. 2012. On the sensitivity of surface NMR in the presence of electrical conductivity anomalies. *Geophysical Journal International* **189**, 331–342.
- Mohnke O. and Yaramanci U. 2005. Forward modeling and inversion of MRS relaxation signals using multi-exponential decomposition. *Near Surface Geophysics* **3**, 165–185.
- Müller-Petke M., Dlugosch R. and Yaramanci U. 2011. Evaluation of surface nuclear magnetic resonance-estimated subsurface water content. *New Journal of Physics* **13**.
- Müller-Petke M. and Yaramanci U. 2008. Resolution studies for Magnetic Resonance Sounding (MRS) using the singular value decomposition. *Journal of Applied Geophysics* **66**, 165–175.
- Müller-Petke M. and Yaramanci U. 2010. QT inversion – Comprehensive use of the complete surface NMR data set. *Geophysics* **75**, WA199–WA209.
- Nyboe N.S., Jørgensen F. and Sørensen K.I. 2010. Integrated inversion of TEM and seismic data facilitated by high penetration depths of a segmented receiver setup. *Near Surface Geophysics* **8**, 467–473.
- Schirov M.D., Legchenko A. and Creer G. 1991. A New Non-invasive Groundwater Detection Technology for Australia. *Exploration Geophysics* **22**, 333–338.
- Schirov M.D. and Rojkowski A.D. 2002. On the accuracy of parameters determination from SNMR measurements. *Journal of Applied Geophysics* **50**, 207–216.
- Tarantola A. and Valette B. 1982. Generalized nonlinear inverse problems solved using an east squares criterion. *Reviews of Geophysics and Space Physics* **20**, 219–232.
- Walsh D.O., Grunewald E., Turner P., Hinnell A. and Ferre P. 2011. Practical limitations and applications of short dead time surface NMR. *Near Surface Geophysics* **9**, 103–111.
